International Journal of Clinical and Experimental Neurology, 2016, Vol. 4, No. 1, 1-8
Available online at http://pubs.sciepub.com/ijcen/4/1/1

DOI:10.12691/ijcen-4-1-1

Age-related Volumetric Changes of Prefrontal Gray and White Matter from Healthy Infancy to Adulthood

Mie Matsui[1,*], Chiaki Tanaka[2], Lisha Niu[1], Kyo Noguchi[3], Warren B. Bilker[4], Michael Wierzbicki[4], Ruben C. Gur[5]

[1]Department of Psychology, Graduate School of Medicine and Pharmaceutical Sciences, University of Toyama, Japan
[2]Department of Pediatrics, Graduate School of Medicine and Pharmaceutical Sciences, University of Toyama, Japan
[3]Department of Radiology, Graduate School of Medicine and Pharmaceutical Sciences, University of Toyama, Japan
[4]Department of Biostatistics and Epidemiology, University of Pennsylvania, Philadelphia, Pennsylvania, USA
[5]Department of Psychiatry, University of Pennsylvania, Philadelphia, Pennsylvania, USA
*Corresponding author: mmatsui@las.u-toyama.ac.jp

Abstract Despite increasing evidence of the role of the prefrontal cortex in providing the neural substrate of higher cognitive function and neurodevelopment, little is known about neuroanatomic changes in prefrontal subregions during human development. In this prospective study, we evaluated prefrontal gray and white matter volume in healthy infants, children, adolescents, and adults. Magnetic resonance imaging was performed on 107 healthy people aged one month to 25 years. Gray and white matter volumes of the dorsolateral, dorsomedial, orbitolateral, and orbitomedial prefrontal cortex were quantified. The results indicated that both children and early adolescents had larger dorsolateral gray matter volume than infants and adults. Dorsolateral white matter volumes in children, early adolescents, and late adolescents were larger than those of infants. Dorsomedial white matter volumes of early adolescents, late adolescents, and adults were also larger than those of infants. There was no significant difference among age groups in both orbital prefrontal regions. These findings suggest that there are two important stages of structural change of the prefrontal cortex from infancy to young adulthood. First, growth spurts of both gray matter and white matter during the first 2 years of life have been shown to occur specifically in the dorsal prefrontal cortex. Second, gray matter changes have been shown to be regionally specific, with changes in the dorsal, but not orbital, prefrontal cortex peaking during late childhood or early adolescence. Thus, developmental differences within sectors of the prefrontal lobe and evidence of neural pruning and myelination may be useful in understanding the mechanisms of neurodevelopmental disorders.

Keywords: *magnetic resonance imaging (MRI), development, prefrontal area, orbitofrontal cortex, dorsolateral prefrontal cortex*

Cite This Article: Mie Matsui, Chiaki Tanaka, Lisha Niu, Kyo Noguchi, Warren B. Bilker, Michael Wierzbicki, and Ruben C. Gur, "Age-related Volumetric Changes of Prefrontal Gray and White Matter from Healthy Infancy to Adulthood." *International Journal of Clinical and Experimental Neurology*, vol. 4, no. 1 (2016): 1-8. doi: 10.12691/ijcen-4-1-1.

1. Introduction

A thorough understanding of human brain development from birth through adolescence to adulthood is essential to our understanding of cognitive development. Studies of normal brain maturation have consistently shown that brain morphology changes dynamically into adulthood [1,2,3,4]. In the past 15 years, significant progress has been made in delineating changes in brain morphology, including those in gray and white matter, from birth to adolescence. The human brain undergoes rapid growth during the first 2 years of life [5]. Gray matter volume reductions between childhood and adolescence with relatively stable total brain volume in this age range have been consistent findings in the literature [3]. This would be expected given postmortem studies that have revealed a protracted progression of myelination, particularly into frontal and parietal regions [6]. Additionally, regressive events, such as reductions in synaptic density and spines, have been reported to occur throughout adolescence in humans [7,8] and in monkeys [9,10]. Magnetic resonance imaging (MRI) studies of human brain maturation during adolescent years have consistently shown subtle increases in total brain volume along with regionally variable patterns of reductions in gray matter volume and increases in total white matter volume [1]. Postmortem studies show that maturational factors occur in a programmed way such that more primitive regions of the brain (e.g., brainstem, cerebellum) mature earlier, and phylogenetically more advanced regions of the brain (e.g., association cortices of the frontal lobes) develop later [6].

Neuropsychological studies show that the frontal lobes are essential for such functions as response inhibition, emotional regulation, planning, and organization [11]. The human prefrontal cortex mediates the highest cognitive capacities, including reasoning, planning, and behavioral control [12]. This relatively large and complex associative brain region has been shown to develop along with other

higher-order association regions as children mature from adolescence into adulthood [13]. Structural neuroimaging studies using growth-mapping techniques suggest that the prefrontal cortex matures more slowly than other regions of the brain [14]. However, little is known about differences in neuroanatomic developmental changes within sectors of the prefrontal cortex in humans.

We previously studied MRI in healthy children aged 1 month to 10 years and found growth spurts of the whole brain, frontal lobes, and temporal lobes during the first 2 years of life [5]. We further extended the age range until the 20s and found that peak volumes occurred around preadolescence [15]. The present study examines the volume of medial and lateral aspects of the dorsal and orbital prefrontal subregions using thin (1-mm) slices and an imaging sequence optimal for gray matter (GM)/white matter (WM) segmentation. (1) We hypothesized that GM development in infancy through early adulthood would be nonlinear as described before, and would progress in a localized, region-specific manner in the prefrontal region. (2) We also predicted that the regions associated with the orbital prefrontal lobe would develop earlier compared with the dorsal prefrontal lobe.

2. Methods

2.1. Participants

Study participants consisted of 107 healthy people with no personal or family history of psychiatric or neurological disorders. Participants included 13 infants (7 boys and 6 girls, aged 1 month to 2 years), 24 children (11 boys and 13 girls, aged 2 to 9 years), 18 early adolescents (7 men and 11 women, aged 10 to 14 years), 36 late adolescents (19 men and 17 women, aged 15 to 19 years), and 16 adults (8 men and 8 women, aged 20 to 25 years). They were recruited by advertisement in our university and in the Kureha region of Toyama city. Their heights and weights were all in the normal range. All subjects had normal neurological development, and had no abnormal findings in routine MRI studies. Nineteen subjects under 6 years of age were sedated with monosodium trichorethyl phosphate syrup (0.5-1.0 ml/kg). This drug was administered one time only; for 5 children who did not fall asleep after the single dose, the study was discontinued. Written informed consent was obtained from adult subjects and the parents of underage subjects before their participation in the study and after the purpose and all procedures of the study were fully explained. This study was approved by the Committee of Medical Ethics of Toyama University.

2.2. MRI Acquisition

The MRIs were acquired on a 1.5-T Magnetom Vision (Siemens Inc., Erlangen, Germany). Axial images were obtained by using a fast low angle shot gradient refocused 3-dimensional (3-D) sequence with the following parameters: flip angle = 35°, repetition time (TR) = 35 msec, echo time (TE) = 6 msec, nex = 1. The image obtained was T1-weighted with a field of view of 256 mm and a matrix size of 256 × 256, and the entire scan was obtained in about 15 min. The slice thickness was 1.0 mm, and 140 to 190 contiguous slices were obtained in each case. Each acquisition was transferred to an on-line UNIX workstation (SUN Microsystems Inc., SPARC20). All image processing was performed by using a semi-automated software package [16]. Brain volume was first extracted by an algorithm [17] with optimal thresholding, morphological operations, and Chamfer distance [18]. This algorithm serves as a presegmentation procedure to estimate and extract a whole 3-D brain volume from the MR image before the segmentation is performed. An adaptive Bayesian algorithm was then applied for segmenting 3-D MRIs into 3 tissue types: GM, WM, and cerebrospinal fluid (CSF) [19,20]. The algorithm models MRIs as collections of regions with slowly varying intensity plus white Gaussian noise. Tissue type is modeled by a Markov random field (MRF) with the 3-D second order neighborhood system, where different potentials are used for in-plane and axial directions to account for anisotropic images. This model is essential for accurate segmentation because it incorporates spatial integration among adjacent label voxels, which reduce degradation due to poor signal-to noise ratio and feature contrast. We introduced a cubic B-spline function to model slowly varying mean intensity of each tissue type through the least squares fitting technique. The spline is desirable for overcoming the “shading” effects and reduces bias against small isolated regions, such as sulcal CSF. Combining spline representation and adaptation makes the segmentation more accurate and robust [21].

2.3. MRI Processing

2.3.1. Manual Delineation of Regions of Interest

Manual delineation of cerebral hemispheres [21] and prefrontal subregions [22] was based on the standard guidelines below.

2.3.1.1. Cerebral Hemispheres

Collection of data in the axial plane required neuroanatomic knowledge to separate the supratentorial from infratentorial compartments. All supratentorial slices were analyzed and the infratentorial CSF and tissue were excluded by placing a boundary around the posterior fossa on each slice. The caudal brain stem structures below the level of the cerebral peduncles of the midbrain were excluded. The hypothalamic and chiasmatic cisterns were retained, but the pituitary, the carotid cistern, the ambient cistern, and the quadrigeminal plates were excluded. Depending on head position, the following was encountered. 1) Occipital lobes often projected onto the same section as the cerebellar hemispheres and brain stem. Because the tentorium slopes, the margins had to be reconciled, and CSF in the superior cerebellar and quadrigeminal cisterns had to be subtracted. 2) The sella turcica was excluded since the enlargements of the CSF space in and around the pituitary gland depended on the intactness of the diaphragma sellae. However, CSF in the chiasmatic cistern was included. 3) Other anatomic variables included the uppermost portion of the midbrain and the cisterns anterior to it. A line was drawn that connected the two cerebral peduncles with the basilar artery, and the brain stem posterior to that was excluded. The most superior portion of the midbrain and the CSF in the chiasmatic cistern anterior to this, along with

structures of the hypothalamus (including the mammillary bodies, tuber cinereum and infundibular stalk, and optic chiasm), were included.

2.3.1.2. Prefrontal Subregions

Subdivisions were derived with neuroradiological and neuroanatomic input, using topographical triangulation and tissue segmentation techniques to maximize the precision and reliability of region delineation. Prefrontal cortex was divided into dorsolateral, dorsomedial, and lateral and medial orbital sectors. Regions were drawn on the sagittal series with 3-D visualization tools (Figure 1).

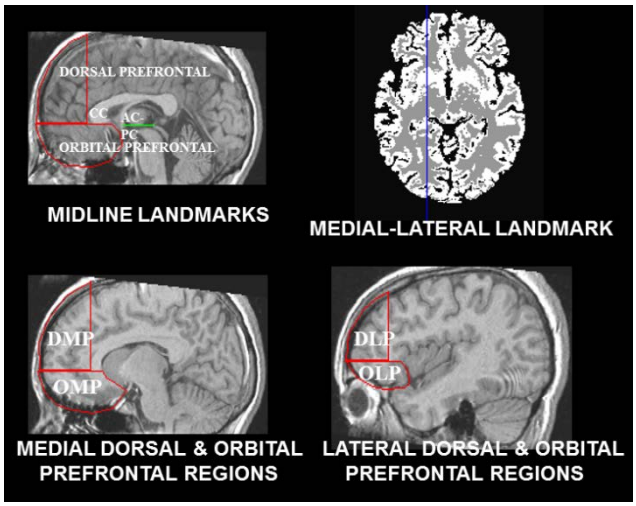

Figure 1. Illustration of region placement for the prefrontal cortex. MRI segmentation is illustrated on the upper right corner, where GM is depicted in white, WM in light gray, and CSF in black. AC-PC indicates anterior commissure–posterior commissure; CC, corpus callosum; DMP, dorsomedial prefrontal; OMP, orbitomedial prefrontal; DLP, dorsolateral prefrontal; and OLP, orbitolateral prefrontal

The prefrontal region for each hemisphere extends from midline to the lateral cortical perimeters. The dorsal and orbital regions are separated by a line drawn at the level of the anterior commissure (AC). This dividing landmark is used throughout the mediolateral extent of the frontal lobe. The inferior genu of the corpus callosum at midline marks the posterior border of the dorsal prefrontal region. The posterior border of the orbitomedial region is a line drawn from coordinates determined by the anterior tip of the corpus callosum and the inferior cortical border at the first appearance of the caudate. Laterally, the posterior border of this region is a line drawn from the head of the caudate. The posterior border of the orbitolateral region is marked by the caudate and the insula. For dorsal and orbital regions, an axial view of the gray-white segmented image is used to determine the border between the medial and lateral regions; they are divided by the medial-most aspect of cortical GM, which runs along the transverse orbital sulcus at the slice superior to the last view of the medial orbital sulcus.

The dorsal prefrontal region includes the frontal pole and frontomarginal, superior frontal, and anterior sections of the middle and inferior gyri; portions of the anterior cingulate may also be included at midline. The lateral portion of the dorsal region includes the lateral aspects of Brodmann areas 8, 9, 45, 46, and dorsolateral aspects of area 10. The medial portion of this region corresponds to the medial aspects of areas 8 and 9, dorsal portions of areas 32 and 24, and dorsomedial aspects of area 10. The orbital prefrontal region includes the rectal, medial orbital, and suborbital gyri; the ventral portion of the mesial superior gyrus; and the anterior, posterior, and lateral orbital gyri. The lateral portion of the orbital region includes area 47, lateral portions of area 11, and inferolateral portions of area 10. The medial portion of the orbital region corresponds to areas 12, 25, medial 11, inferomedial 10, and ventral 32 and 24.

2.3.1.3. Reliability of Regional volumetric Measurements

The interrater reliability was examined in a sample of 10 randomly selected brain scans analyzed by three raters (L.N., C.T., M.M.). The intraclass correlation (ICC) for total cerebral volumes ranged from 0.95 to 0.98, and those of prefrontal volumes ranged from 0.88 to 0.96. The intrarater reliability was also examined in the same 10 scans analyzed by two of these raters (L.N. and C.T.), and the correlation for total cerebral volume and prefrontal volumes ranged from 0.90 to 0.97. The raters (L.N. and C.T.) then completed the analysis on the remaining scans.

2.4. Statistical Analyses

We fit an additive model to each region on age, adjusting for total volume in gray/white. Additive models are generalizations of the classical linear model. For the classical linear model, we model:

$$Y = \alpha + \sum_{i=1}^{p} \beta_i X_i + \varepsilon$$

where the errors have zero mean and constant variance, are independent of the covariates, and the β s are scalars. Conversely, the additive model is modeled by:

$$Y = \alpha + \sum_{i=1}^{p} f_i(X_i) + \varepsilon$$

where the errors are defined as above. Whereas in the classical linear model, the f s are linear functions, the f s in the additive model are arbitrary univariate smooth functions. The smooth functions are estimated simultaneously using a backfitting algorithm [23]. The models were fit using the gam() function in the mgcv package in R statistical package [24].
Thus, the model we fit was the following:

$$[\text{Model 1}]: \; RBV = \alpha + f_1(x_1) + f_2(x_2) + \varepsilon$$

where RBV is the brain volume of a particular region, or regional brain volume. $f_1(x_1)$ represents the contribution to RBV for each month of age, adjusted for total gray (or white) volume in the brain. Likewise, $f_2(x_2)$ represents the contribution to RBV for each ml of total gray (or white) volume in the brain, adjusted for age. An interaction between age and total gray (or white) volume was tested for, and found not to be significant in each region. We also modeled total GM, total WM, and total CSF on age using additive models.

To examine age effects and sex differences on hemispheric whole-brain and regional volumes, we used age as a grouping factor by dividing the participants into infants (age < 2 years), children (2-9 years), early

adolescents (10-14 years), late adolescents (15-19 years), and adults (age 20-25 years), and performed a multivariate repeated-measures analysis of variance (MANOVA) [25]. Sex was another grouping factor, and GM vs. WM and Hemisphere were repeated-measures (within-group) factors. Post-hoc Tukey's tests were employed to follow up the significant main effects or interactions yielded by MANOVA. In addition, statistical differences in the prefrontal subregional volume measures were also analyzed with repeated-measures multivariate analysis of covariance (MANCOVA) with whole brain volume as a covariate for each region, and with age group and sex as between-group factors; GM vs. WM and Hemisphere were repeated-measures (within-group) factors. Post-hoc Tukey's tests were employed to follow up the significant main effects or interactions yielded by MANCOVA.

3. Results

3.1. Whole Brain

Figure 2 is a plot of the predicted volume of total GM, total WM, and total CSF by age. All three regions exhibit a bend in the curve in the window of 50-75 months of age. Since these bends are of interest, we wished to find confidence intervals for these aspects of the curves. We accomplished this as follows. We bootstrapped the data 1000 times. At each iteration, we fit model 1 and we calculated the numerical first and second derivatives of the predicted curves. Since we were interested in where the slopes of the curves change the most, we found the age at which the second derivative is at an extrema. Using these 1000 values of age, we constructed a 95% confidence interval for point of the bend.

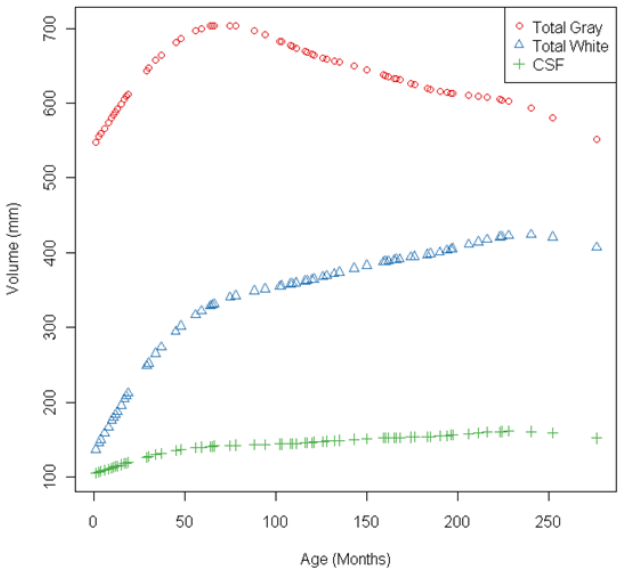

Figure 2. Plot of the predicted volume of total GM, total WM, and total CSF by age

CSF, cerebrospinal fluid
All three regions exhibit a bend in the curve in the window of 50-75 months of age. This shows the change in GM and WM volume is large during this period.

The (age group × sex × GM vs. WM × Hemisphere) MANOVA for the whole-brain values, presented in Table 1, showed a main effect of age group, $F(4,97) = 22.78$, $p < 0.0001$, with infants having overall smaller volumes than all age groups. There were also main effects for the within-group (repeated-measures) factors. GM volumes were larger than WM, $F(1, 97) = 3134.50$, $p < 0.0001$, and right hemispheric volumes were overall larger than left, $F(1,97) = 34.52$, $p < 0.0001$. Men had larger volumes than women, $F(1,97) = 17.14$, $p < 0.0001$. However, these main effects were qualified by higher order interactions. GM vs. WM × age, $F(4,97) = 98.62$, $p < 0.0001$, indicated that there were different patterns between GM and WM among the age groups. Post-hoc analyses showed infants had smaller GM volumes than children ($p < 0.001$) and early adolescents ($p < 0.05$), children had larger GM volumes than late adolescents ($p < 0.01$) and adults ($p < 0.001$), and early adolescents had larger GM volumes than adults ($p < 0.05$). Thus, GM shows an increase from infancy to childhood, followed by decline. On the other hand, infants had smaller WM volumes than all age groups (all, $p < 0.001$), and children had smaller WM volumes than late adolescents ($p < 0.001$) and adults ($p < 0.001$). Thus, WM shows a steady increase from infancy to adulthood. A GM vs. WM × sex interaction, $F(1,97) = 6.02$, $p = 0.016$, indicated that the main effect of larger volume of men came from GM, but not WM. A GM vs. WM × hemisphere interaction, $F(1,97) = 19.74$, $p < 0.0001$, indicated that the main effect of larger right hemispheric volumes came entirely from WM, while GM is symmetric and even slightly larger on the left. A GM vs. WM × age group × sex interaction, $F(4,97) = 2.47$, $p < 0.05$, indicated that differences between men and women were relatively large for GM volume by age group, but not for WM volume. No other interaction approached significance.

Table 1. Summary Table for the MANOVA of whole brain

Source	F	p-value
Age group	**22.779**	**<0.0001**
Sex group	**17.14**	**<0.0001**
GW	**3134.499**	**<0.0001**
Hemisphere	**34.523**	**<0.0001**
Age group*Sex	1.306	0.2734
GW*Age group	**98.62**	**<0.0001**
GW*Sex	**6.02**	**0.016**
Hemisphere*Age group	0.665	0.618
Hemisphere*Sex	0.272	0.6029
GW*Hemisphere	**19.744**	**<0.0001**
GW*Age group*Sex	**2.468**	**0.0498**
Hemisphere*Age group*Sex	0.569	0.686
GW*Hemisphere*Age group	2.194	0.0753
GW*Hemisphere*Sex	2.238	0.1379
GW*Hemisphere*Age group*Sex	1.002	0.4105

Abb.: GW= Gray versus White matter contrast.

3.2. Prefrontal Volumes

The distributions by age of GM and WM volumes are shown in Figure 3. Figure 4 is a plot of the predicted RBV of GM (or WM) by age, adjusted for total GM (or WM) for both the dorsal regions and the orbital regions. For the prefrontal regions, the bend of interest is also an extrema. Thus, we followed the same procedure as above for the

whole brain with a slight alteration. We again bootstrapped the data 1000 times. At each iteration, we fit model 1, and calculated the predicted values of RBV across age at the mean of gray (or white) total. We calculated the numerical first derivative and found the maximum and/or minimum of the predicted curve by interpolating the root of the first derivative curve. Using the 1000 extrema, we calculated 95% confidence intervals for the maximum and/or minimum. Table 2 shows the mean of the 1000 age values for the bend(s) plus 95% confidence intervals in prefrontal regions.

Table 2. The mean of the 1000 age values for the bend(s) plus 95% confidence intervals in prefrontal regions.

Region	Mean (month)	CI
GDL	145.0	85.6-204.3
GDM	151.7	106.9-196.4
GOL	162.2	116.8-207.5
GOM	162.4	139.4-185.3
WDL	122.7	45.1-200.3
WDM maximum	102.9	18.9-186.9
WDM minimum	165.8	46.5-285.2
WOL	167.9	138.8-197.0
WOM	171.8	143.1-200.4

GDL = gray dorsolateral, GDM = gray dorsomedial, GOL = gray orbitolateral, GOM = gray orbitomedial, WDL = white dorsolateral, WDM = white dorsomedial, WOL = white orbitolateral, WOM = white orbitomedial.

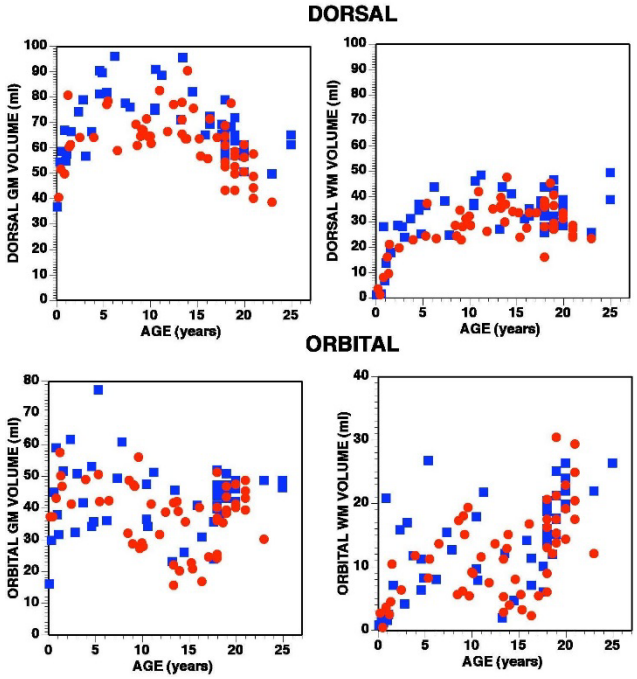

Figure 3. The distributions by age of GM and WM volumes

Blue squares show men and red circles show women.
Left upper plots show dorsal GM volume and right upper plots show dorsal WM volume. Left lower plots show orbital GM volume and right lower plots show orbital WM volume. Plots representing dorsal distribution differ significantly from orbital plots.

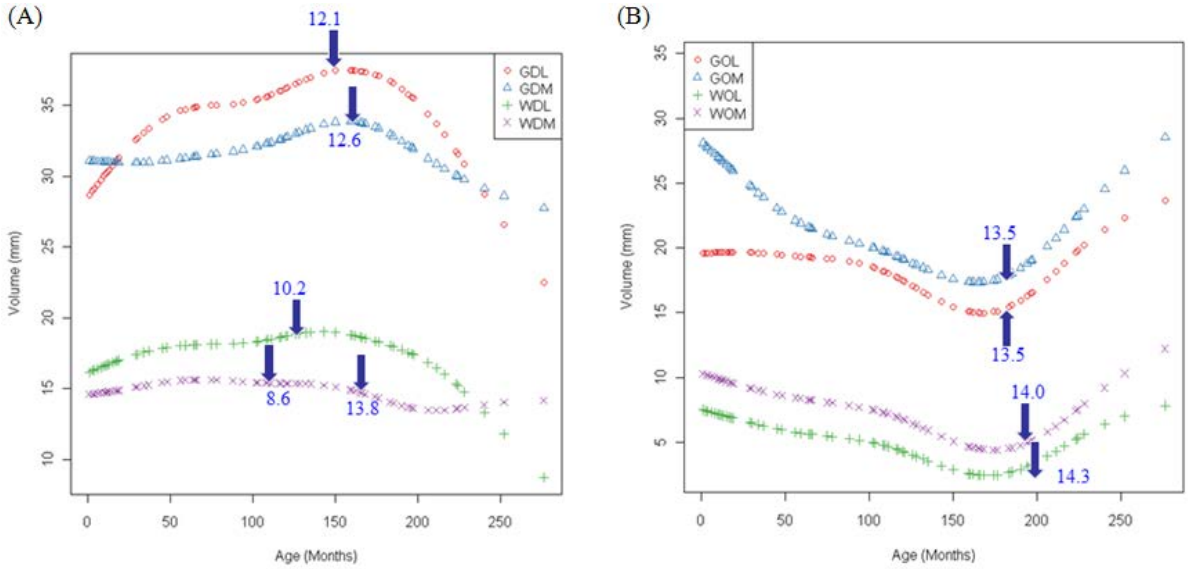

Figure 4. Plot of the predicted RBV of GM (or WM) by age, adjusted for total GM (or WM) for the dorsal regions (A) and the orbital regions (B)

GDL = gray dorsolateral, GDM = gray dorsomedial, WDL = white dorsolateral, WDM = white dorsomedial.
Blue numbers and arrows on lines show peak ages (years old).

The result of the MANOVA applied to the prefrontal volumes (age group × sex × GM vs. WM × hemisphere × prefrontal regions) is summarized in Table 3. Following the MANOVA, the main effect for age group demonstrates that infants had overall smaller volumes than every group, the GM vs. WM effect indicates larger GM values, the main effect for sex indicated that men had larger volumes than women, and the main effect for hemisphere reflects larger values on the right than the left hemisphere across regions, groups, and compartments. The main effect of prefrontal volumes indicates volumes were in the order of dorsolateral > dorsomedial > medial orbital > lateral orbital prefrontal region. Following the MANCOVA, there were no main effects of sex, GM vs. WM, and Hemisphere. These main effects were qualified by several higher order interactions. The prefrontal regions × age interaction indicated greater differences among age groups in dorsolateral and dorsomedial regions than medial orbital and lateral orbital prefrontal regions. Infants also had smaller dorsomedial volume than children and early adolescents. The prefrontal regions × sex interaction indicated men had larger dorsolateral volume than women, but there was no sex difference in any other region. GM vs. WM × age group indicated there were different age effects between GM and WM. That is, children had larger GM volume than infants, late

adolescents, or adults, while infants had smaller WM volume than children, early adolescents, late adolescents, or adults. A GM vs. WM × prefrontal interaction indicated both GM and WM volume were in the order of dorsolateral > dorsomedial > medial orbital > lateral orbital prefrontal region. A GM vs. WM × age group × sex interaction indicated that the main effect of children was larger GM volume than infants and late adolescents for men, while WM volumes of early adolescents, late adolescents, and adults of both sexes were larger than those of infants. Finally, a GM vs. WM × prefrontal region × age group interaction indicated that the differences among age groups were relatively showed for dorsolateral prefrontal GM volumes and both dorsolateral and dorsomedial prefrontal WM volumes (Figure 5). That is, both children and early adolescents had larger dorsolateral GM volumes than infants and adults. Dorsolateral WM volumes of children, early adolescents, and late adolescents were larger than those of infants. In addition, dorsomedial WM volumes of early adolescents, late adolescents, and adults were larger than those of infants. There was no significant difference among age groups in both orbital prefrontal regions. The above interactions of MANOVA were also found in the results of MANCOVA.

Table 3. Summary Table for the MANOVA of prefrontal volumes

Source	F	p-value
Age group	12.235	<0.0001
Sex group	13.819	0.0004
Region	264.051	<0.0001
GW	3583.708	<0.0001
Hemisphere	15.234	0.0002
Age group*Sex	1.338	0.2613
Region*Age group	13.122	<0.0001
Region*Sex	3.424	0.0176
GW*Age group	47.554	<0.0001
GW*Sex	5.02	0.0273
GW*Region	75.501	<0.0001
Hemisphere*Age group	0.632	0.641
Hemisphere*Sex	0.074	0.7866
Hemisphere*Region	63.379	<0.0001
GW*Hemisphere	50.061	<0.0001
Region*Age group*Sex	0.885	0.5623
GW*Age group*Sex	2.886	0.0263
GW*Region*Age group	11.744	<0.0001
GW*Region*Sex	1.182	0.317
Hemisphere*Age group*Sex	0.388	0.817
Hemisphere*Region*Age group	1.249	0.2488
Hemisphere*Region*Sex	0.338	0.7978
GW*Hemisphere*Age group	0.66	0.6214
GW*Hemisphere*Sex	1.311	0.2551
GW*Hemisphere*Region	5.238	0.0016
GW*Region*Age group*Sex	1.148	0.3208
GW*Hemisphere*Age group*Sex	0.296	0.8799
GW*Hemisphere*Region*Age group	3.082	0.0004
GW*Hemisphere*Region*Sex	0.874	0.4547
GW*Hemisphere*Region*Age group*Sex	1.2	0.2821

Abb.: GW= Gray versus White matter contrast.

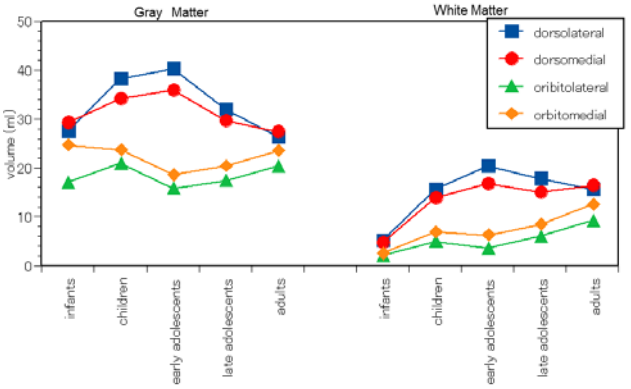

Figure 5. Means of compartmental volumes (in milliliters) for age groups for 4 prefrontal subregions. Left: GM, Right: WM

A GM vs. WM × prefrontal regions × age group interaction indicated that the differences among age groups were relative for dorsolateral prefrontal GM volume and both dorsolateral and dorsomedial prefrontal WM volumes. Both children and early adolescents had larger dorsolateral GM volumes than infants and adults. Dorsolateral WM volumes of children, early adolescents, and late adolescents were larger than those of infants. Dorsomedial WM volumes of early adolescents, late adolescents, and adults were larger than those of infants. There was no significant difference among age groups in both orbital prefrontal regions.

4. Discussion

This study reported whole-brain and regional prefrontal volume changes from infancy to adulthood. Regarding whole-brain volume, the results showed that GM volume increases during infancy and childhood, and decreases in adolescence before adulthood. On the other hand, WM volume continues to increase from infancy to adulthood. These results were also applied to total prefrontal volume and were consistent with previous MRI reports on whole-brain volume [1,3,4,26]. That is, MRI studies of human brain maturation during adolescent years have consistently shown subtle increases in total brain volume along with regionally variable patterns of reduction in GM volume and increases in total WM volume. Several authors have reported nonlinear changes in cortical GM, with overall decreases of 23% to 32% between the ages of 4 and 30 years [27,28]. The present results showed changes in whole-brain GM volume, with overall decreases of 14.8%, and in WM volume, with increases of 33.2%, between childhood (mean age of 6.3 years) and adulthood (mean age of 21.0 years). Similarly, changes in prefrontal cortex GM volume showed overall decreases of 16.7%, and WM volume showed increases of 30.1%, between childhood and adulthood. Giedd et al. [1] examined MRIs in subjects aged 4 to 22 years and found that GM in the frontal lobe increased during preadolescence, with maximum size attained at 12.1 years for males and 11.0 years for females. The results of the present study are consistent, and showed peaks of GM volume during early adolescence (12 to 13 years) in the prefrontal cortex.

Furthermore, in this study, GM and WM volumes of the dorsolateral, dorsomedial, orbitolateral, and orbitomedial prefrontal cortex were quantified. The results indicated that both children and early adolescents had larger dorsolateral GM volume than infants and adults. Dorsolateral WM volumes of children, early adolescents, and late adolescents were larger than those of infants. In

addition, dorsomedial WM volumes in early adolescents, late adolescents, and adults were larger than those of infants. On the other hand, there was no significant difference among age groups in orbital prefrontal regions. GM changes have been shown to be regionally specific, with changes in the dorsal prefrontal lobe peaking during late childhood or early adolescence. In addition, growth spurts of both GM and WM during the first 2 years of life have been shown to occur specifically in the dorsal prefrontal, but not orbital, cortex. These results suggest that major dynamic and regionally specific changes at the two stages are occurring in structures of the prefrontal cortex from infancy through adolescence. However, the volume of the orbital prefrontal cortex does not remain constant. Previous postmortem and neuroimaging studies have suggested that anatomic reorganization of the frontal lobes occurs in synaptic density count, myelination, dendritic arborization, and in vivo global volumetric and cortical complexity during this age range. Jernigan et al. [29] hypothesized that the reductions they observed in dorsal cortical volume were related to decreases in synaptic density found during the same age range in human autopsy material [30]. Thus, the present results suggest that regressive (i.e., synaptic pruning) and progressive (i.e., myelination) cellular events occur simultaneously in the prefrontal cortex after childhood, both of which could result in the appearance of GM density reduction on MRI, as Sowell et al. [31] pointed out. Myelination is recognized from infancy and the most dorsal regions of the brain responsible for higher cognitive functions may continue the process well into adolescence. Dorsal and orbital cortices do not ultimately myelinate to the same degree: on average, the dorsal cortex is more myelinated than the orbital cortex.

That may be why different subregions of the prefrontal cortex have different connections. Thus, a general topological pattern of connectivity can be recognized, particularly in primates. The orbital prefrontal cortex is primarily connected to the medial thalamus, the hypothalamus, the ventromedial caudate, and the amygdala. The dorsolateral prefrontal cortex, on the other hand, is primarily connected to the lateral thalamus, the dorsal caudate nucleus, the hippocampus, and the neocortex [12]. Research on the cyto- and myeloarchitecture of the developing prefrontal cortex in primates suggests that its orbital areas mature earlier than the areas of the dorsolateral prefrontal convexity [12]. The dorsal and lateral areas undergo later development and further differentiation than the medial and ventral areas.

Our results showed that women had smaller whole-brain volumes than men, as most previous studies have shown [21,32]. Our previous study failed to observe any significant variation between sexes in infants and children [5]. This study added more extended age, so that sex differences clearly appeared from early adolescence to adulthood. In postmortem and imaging studies of adult brains, authors consistently point out gender differences in total brain volume, with adult males having, on average, a 10% greater volume than females [2,21,27,33,34,35], while women have a higher proportion of GM relative to cranial volume [21]. Reiss et al. [28] reported that the first appearance of gender differences in brain volume had been recognized in children as young as 5 years of age.

Our study has several important limitations. The study is cross-sectional, and longitudinal investigation of prefrontal development is required to support the present results. Second, the present findings of structural changes in the lateral prefrontal cortex may accompany the emergence of executive functions such as abstract reasoning and planning that occur during adolescence. In the future, we will need to investigate the relationship between prefrontal function and structure. Finally, knowledge of the course of normal brain development must provide the foundation for the recognition of pathologic brain development such as schizophrenia. Morphologic changes in the present study may also relate to pubertal alterations of higher cognitive and affective functions, or to the decrease in cortical plasticity thought to occur during late childhood and adolescence [22].

In summary, our findings suggest that there are two important stages of structural change in the prefrontal cortex from infancy to young adulthood. First, growth spurts of both GM and WM during the first 2 years of life have been shown to occur specifically in the dorsal prefrontal, but not orbital, cortex. Second, GM changes have been shown to be regionally specific, with changes in the dorsal prefrontal cortex peaking during late childhood or early adolescence. These findings may have some implications for understanding the mechanisms underlying neurodevelopmental disorders.

Acknowledgement

This study was supported by a Grant-in-Aid for Scientific Research (B) 20330141, 26285155, Grand-in-Aid for Exploratory Research 26590143 and Grant-in-Aid for Scientific Research on Innovative Areas 26118707 from the Japan Society for the Promotion of Science (JSPS).

References

[1] Giedd JN, Blumenthal J, Jeffries NO, Castellanos FX, Liu H, Zijdenbos A, Paus T, Evans AC, Rapoport JL (1999) Brain development during childhood and adolescence: a longitudinal MRI study. *Nature Neurosci* 2:861-863.

[2] Dekaban A, Sadowsky D (1978) Changes in brain weights during the span of human life: relation of brain weights to body heights and body weights. *Ann Neurol* 4:345-356.

[3] Toga AW, Thompson PM, Sowell ER. (2006) Mapping brain maturation. *Trends Neurosci* 29:148-159.

[4] Paus T, Keshavan M, Giedd JN. (2008) Why do many psychiatric disorders emerge during adolescence? *Nat Rev Neurosci* 9:947-957.

[5] Matsuzawa J, Matsui M, Konishi T, Noguchi K, Gur RC, Bilker W, Miyawaki T. (2001) Age-related volumetric changes of brain gray and white matter in healthy infants and children. *Cereb Cortex* 11:335-342.

[6] Yakovlev PL, Lecours AR (1967) The myelogenetic cycles of regional maturation of the brain. In: *Resional development of the brain in early life* (Minkowski A, eds), pp 3-70. Oxford: Blackwell.

[7] Huttenlocher PR (1990) Morphometric study of human cerebral cortex development. *Neuropsychologia* 28:517-527.

[8] Huttenlocher PR, Dabholkar AS (1997) Regional differences in synaptogenesis in human cerebral cortex. *J Comp Neurol* 387: 167-178.

[9] Peters A, Sethares C, Luebke JI. (2008) Synapses are lost during aging in the primate prefrontal cortex. *Neuroscience* 152:970-981.

[10] Elston GN, Oga T, Fujita I (2009) Spinogenesis and pruning scales across functional hierarchies. J Neurosci 29:3271-3275.

[11] Stuss DT, Benson DF (1986) *The frontal lobes*. New York: Raven Press.

[12] Fuster JM (1997) *The prefrontal cortex*. Third edition. Philadelphia: Lippincott-Raven Publishers.

[13] Fuster JM (2002) Frontal lobe and cognitive development. *J Neurocytol* 31:373-385.

[14] Gogtay N, Giedd JN, Lusk L, Hayashi KM, Greenstein D, Vaituzis AC, Nugent TF 3rd, Herman DH, Clasen LS, Toga AW, Rapoport JL, Thompson PM. (2004) Dynamic mapping of human cortical development during childhood through early adulthood. *Proc Natl Acad Sci* 101:8174-8179.

[15] Tanaka C, Matsui M, Uematsu A, Noguchi K, Miyawaki T. (2012) Developmental trajectories of the fronto-temporal lobes from infancy to early adulthood in healthy individuals. *Dev Neurosci* 34: 477-487.

[16] Kohn MI, Tanna NK, Herman GT, Resnick SM, Mozley PD, Gur RE, Alavi A, Zimmerman RA, Gur RC. (1991) Analysis of brain and cerebrospinal fluid volumes with MR imaging. *Radiology* 178:115-22.

[17] Yan MXH, Karp JS (1994a) Image registration of MR and PET based on surface matching and principal axes fitting. *Proc IEEE Med Imaging Conf* 4:1677-1681.

[18] Borgefors G (1986) Distance transformations in digital images. *Comput Vis Graph Image Process* 34:344-371.

[19] Yan MXH, Karp JS (1994b) Segmentation of 3D brain MR using an adaptive K-means clustering algorithm. *Proc IEEE Med Imaging Conf* 4: 1529-1533.

[20] Yan MXH, Karp JS (1995) An adaptive bayesian approach to three-dimensional MR brain segmentation. In: *Information processing in medical imaging* (Bizais Y, Barillot C, Di Paola R, eds), pp 201-213. Dordrecht: Kluwer Academic Publishers.

[21] Gur RC, Turetsky BI, Matsui M, Yan M, Bilker W, Hughett P, Gur RE (1999) Sex differences in brain gray and white matter in adults: correlation with cognitive performance. *J Neurosci* 19: 4065-4072.

[22] Gur RE, Cowell PE, Latshaw A, Turetsky BI, Grossman RI, Arnold SE, et al (2000). Reduced dorsal and orbital prefrontal gray matter volumes in schizophrenia. *Arch Gen Psychiatry* 57: 761-768.

[23] Hastie, T.J., Tibshirani, R.J. (1990) *Generalized Additive Models.* London: Chapman and Hall, Print.

[24] Wood, SN. (2006). *Generalized Additive Models: An Introduction with R.* Boca Raton, FL: Chapman and Hall/CRC, Print.

[25] Maxwell WE, Delaney HD (1990) *Designing experiments and analyzing data: a model comparisons approach.* Belmont, CA: Wadsworth.

[26] Durston S, Hulshoff Pol HE, Casey BJ, Giedd JN, Buitelaar JK, van Engeland H. (2001) Anatomical MRI of the developing human brain: what have we learned? *J Am Acad Child Adolesc Psychiatry* 40:1012-1020.

[27] Pfefferbaum A, Mathalon DH, Sullivan EV, Rawles JM, Zipursky RB, Lim KO (1994) A quantitayive magnetic resonance imaging study of changes in brain morphology from infancy to late adulthood. *Arch Neurol* 51:874-887.

[28] Reiss AL, Abrams MT, Singer HS, Ross JL, Denckla MB (1996) Brain development, gender and IQ in children: a volumetric imaging study. Brain 119:1763-1774.

[29] Jernigan TL, Trauner DA, Hesselink JR, Tallal PA (1991) Maturation of human cerebrum observed in vivo during adolescence. *Brain* 114:2037-2049.

[30] Huttenlocher PR (1979) Synaptic density in human frontal cortex: developmental changes and effects of aging. *Brain Res* 163: 195-205.

[31] Sowell ER, Thompson PM, Tessner KD, Toga AW. (2001) Mapping continued brain growth and gray matter density reduction in dorsal frontal cortex: Inverse relationships during postadolescent brain maturation. *J Neurosci* 21: 8819-8829.

[32] Lenroot RK, Gogtay N, Greenstein DK, Wells EM, Wallace GL, Clasen LS, Blumenthal JD, Lerch J, Zijdenbos AP, Evans AC, Thompson PM, Giedd JN. (2007) Sexual dimorphism of brain developmental trajectories during childhood and adolescence. *Neuroimage* 36:1065-1073.

[33] Ho KC, Roessmann U, Straumfjord JV, Monroe G (1980) Analysis of brain weight. 1. Adult brain weight in relation to sex, race, and age. *Arch Pathol Lab Med* 104: 635-639.

[34] Filipek PA, Richelme C, Kennedy DN, Caviness VS Jr (1994) The young adult human brain: an MRI-based morphometric analysis. *Cereb Cortex* 4: 334-360.

[35] Blatter DD, Bigler ED, Gale SD, Johnson SC, Anderson CV, Burnett BM (1995) Quantitative volumetric analysis of brain MR: normative database spanning 5 decades of life. *Am J Neuroradiol* 16: 241-251.